SCIENTIFIC REPORTS

OPEN

Anti-microRNA screen uncovers miR-17 family within miR-17~92 cluster as the primary driver of kidney cyst growth

Received: 20 June 2018
Accepted: 28 December 2018
Published online: 13 February 2019

Matanel Yheskel, Ronak Lakhia, Patricia Cobo-Stark, Andrea Flaten & Vishal Patel

Autosomal dominant polycystic kidney disease (ADPKD) is the leading genetic cause of renal failure. We have recently shown that inhibiting miR-17~92 is a potential novel therapeutic approach for ADPKD. However, miR-17~92 is a polycistronic cluster that encodes microRNAs (miRNAs) belonging to the miR-17, miR-18, miR-19 and miR-25 families, and the relative pathogenic contribution of these miRNA families to ADPKD progression is unknown. Here we performed an *in vivo* anti-miR screen to identify the miRNA drug targets within the miR-17~92 miRNA cluster. We designed anti-miRs to individually inhibit miR-17, miR-18, miR-19 or miR-25 families in an orthologous ADPKD model. Treatment with anti-miRs against the miR-17 family reduced cyst proliferation, kidney-weight-to-body-weight ratio and cyst index. In contrast, treatment with anti-miRs against the miR-18, 19, or 25 families did not affect cyst growth. Anti-miR-17 treatment recapitulated the gene expression pattern observed after miR-17~92 genetic deletion and was associated with upregulation of mitochondrial metabolism, suppression of the mTOR pathway, and inhibition of cyst-associated inflammation. Our results argue against functional cooperation between the various miR-17~92 cluster families in promoting cyst growth, and instead point to miR-17 family as the primary therapeutic target for ADPKD.

Autosomal dominant polycystic kidney disease (ADPKD), caused by mutations in either *PKD1* or *PKD2*, is one of the most common monogenetic disorders and the leading genetic cause of end-stage renal disease (ESRD) in the United States[1–3]. This condition is characterized by the presence of numerous fluid-filled cysts originating from renal tubules. Excessive proliferation of mutant epithelial cells causes the cysts to expand eventually leading to impairment of normal kidney function.

microRNAs (miRNAs) are small, 22-nucleotide long, non-coding RNAs that post-transcriptionally inhibit mRNA expression[4]. Watson-Crick base-pairing between the seed sequence, a stretch of 6 nucleotides (2 through 8) at 5′ end of a mature miRNA, and a complementary sequence on target mRNA results in the repression of that mRNA[5]. miRNAs that harbor the same seed are classified into one family. miRNAs belonging to one family have redundant biological functions because they target the same mRNAs. In diseases such as cancer[6–9], and as we have recently shown in ADPKD[10,11], aberrant activation of miRNAs can drive disease progression. Accordingly, synthetic oligonucleotides known as anti-miRs have emerged as a novel therapeutic platform to inhibit pathogenic miRNAs[12,13]. Anti-miRs harbor complementary sequences and Watson-Crick base pair with cognate miRNAs thereby sterically hindering their function[14]. In general, anti-miRs have a long half-life (>21 days) and are delivered primarily to the liver and kidney making them attractive therapeutic agents to treat chronic diseases such as ADPKD.

We have previously shown that transgenic overexpression of the miR-17~92 cluster in normal kidneys is sufficient to produce cysts[10]. Conversely, expression of the miR-17~92 cluster is increased in human and murine ADPKD, and its deletion reduced cyst burden in four orthologous mouse models of ADPKD[15]. Based on this work there is a growing interest to develop anti-miR drugs targeting the miR-17~92 cluster as therapeutic agents for ADPKD[16–21]. However, several important questions still need to be addressed before a human-grade, anti-miR drug for ADPKD can be developed. First, miR-17~92 is a complex polycistronic cluster that encodes 6 individual miRNAs (miR-17, miR-18a, miR-19a, miR-20a, miR-19b-1, and miR-92a-1), and which of these miRNAs should

Dallas, Univ Texas Southwestern Med Ctr, 5323 Harry Hines Blvd., F5.206, Dallas, 75390-8856, Texas, USA. Correspondence and requests for materials should be addressed to V.P. (email: vishald.patel@utsouthwestern.edu)

be the focus of drug development is not known. Further complicating drug development, the mammalian genome encodes two additional paralogous clusters known as miR-106a~363 and miR-106b~25. The miR-106a~363 encodes 6 miRNAs (miR-106a, miR-18b, miR-20b, miR-19b-2, miR-92a-2, and miR-363) and the miR-106b~25 cluster encodes 3 (miR-106b, miR-93, and miR-25). miR-92b is independently transcribed[22]. Collectively, the miRNAs encoded from these four loci can be categorized into 4 miRNA families: miR-17, miR-18, miR-19, and miR-25[23]. The primary goal of the current study was to define the relative pathogenic contribution of each miRNA family to ADPKD progression. The second question is while anti-miR-17 treatment slows cyst growth caused due to *Pkd2* mutations whether it will have similar beneficial effects in the setting of *Pkd1* mutations is not known. This is a critical issue considering that nearly 80% of ADPKD patients harbor *PKD1* mutations. Finally, we have shown that cyst-reducing effects of miR-17~92 genetic deletion is attributed to improved cyst metabolic pathways. Whether anti-miRs targeting the miR-17~92 cluster also affect these pathways is unknown.

To address these questions, we used anti-miRs to selectively inhibit the expression of each miRNA family in an orthologous *Pkd1*-KO model of ADPKD. We report that only the inhibition of miR-17 family, but not the miR-18, miR-19, or miR-25 families, attenuates cyst growth. Similar to genetic miR-17~92 deletion, we found that inhibition of the miR-17 family improved mitochondrial metabolism and cyst-associated inflammation. In addition, anti-miR-17 treatment provided the additional benefit of reducing mTOR signaling. These data suggest that, within the miR-17~92 cluster, the miR-17 family is the primary therapeutic target for ADPKD.

Results

Expression of miRNAs produced by the miR-17~92 and related clusters in ADPKD mouse model. We used the KspCre/*Pkd1*$^{F/RC}$ (*Pkd1*-KO) mouse model for our studies. *Pkd1*-KO is an orthologous ADPKD model that harbors a germline hypomorphic *Pkd1* mutation (R3277C)[24] on one allele and *loxP* sites flanking *Pkd1* exons 2 and 4 on the other. We used KspCre-mediated recombination to produce a compound mutant mouse with a kidney-specific null mutation on one allele and a hypomorphic mutation on the other. This is aggressive but a long-lived model of ADPKD with a median survival of about 6 months[15]. We began by comprehensively analyzing the expression levels of each mature miRNA encoded by the miR-17~92, miR-106a~363, and miR-106b~25 clusters in kidneys of *Pkd1*-KO mice at 3 weeks of age. Quantitative real-time PCR (Q-PCR) analysis revealed that five of the six mature miRNAs derived from the miR-17~92 cluster were upregulated in cystic kidneys compared to control kidneys (Fig. 1A). miR-17 and miR-18a were the most upregulated showing an increase in expression by 133.2% and 142.9%, respectively. The expression of miR-19a, miR-20a, and miR-19b was increased by 43.6%, 46.7%, and 29.3%, respectively. miR-92a expression was unchanged. All mature miRNAs derived from the miR-106b~93 cluster were also upregulated. Expression of miR-106b was increased by 45.5%, miR-25 by 37.2%, and miR-93 by 29.4% in cystic kidneys compared to control kidneys (Fig. 1B). miR-92b is transcribed independently, and its expression was increased by 66.9% (Fig. 1C). miRNAs derived from the miR-106a~363 cluster exhibited more variable expression (Fig. 1D). miR-106a level was increased by 51.2% whereas miR-18b, miR-20b, and miR-363 levels were decreased by 53.8%, 63.9%, and 59.4%, respectively. Thus, five out of six miRNAs belonging to the miR-17 family, one out of two miRNAs belonging the miR-18 family, both miRNAs belonging to the miR-19 family, and two of four miRNAs belonging to the miR-25 family were upregulated in cystic kidneys compared to control kidneys.

Anti-miRs specifically inhibit cognate miRNA family without affecting the expression of unrelated miRNAs. We used 12 to 16 nucleotides long, locked nucleic acid-modified anti-miRs to selectively inhibit either the miR-17, miR-18, miR-19, or miR-25 family. Anti-miRs were designed to Watson-Crick base pair with the majority but not the entire length of cognate mature miRNA sequence. The nucleotide sequences of anti-miRs used in the current study are shown in Supplementary Table 1. A mixture of five anti-miRs was used to inhibit all six miR-17 family members simultaneously. Each anti-miR in the mix harbored a perfectly complimentary sequence to the seed sequence (shown in bold in Supplementary Table 1) of miR-17 family. However, the flanking nucleotide sequences were slightly modified to account for minor differences in the sequences of the various miR-17 family members. Using a similar strategy, we designed three anti-miRs that collectively targeted all four miR-25 family members and two anti-miRs that simultaneously targeted the two miR-19 family members. Finally, since the two miR-18 family members have a nearly identical sequence, we used one anti-miR to simultaneously inhibit both members.

Pkd1-KO mice were randomly assigned to receive either PBS, anti-miR-17, anti-miR-18, anti-miR-19, or anti-miR-25 mixtures. A dose of 20 mg/kg per injection was administered intraperitoneally at P10, P11, P12, and P15, and mice were sacrificed at P18. Each mouse injected with an anti-miR cocktail was internally controlled with at least one littermate receiving PBS, thus leading to a PBS control group with a larger sample size. Q-PCR analysis showed that anti-miR mixture targeting the miR-17 family reduced expression of all miR-17 family members but did not affect the expression of miR-18a, miR-19a, or miR-25 (Fig. 2A, Supplementary Fig. 1A). Similarly, treatment with anti-miR-18, anti-miR-19, and anti-miR-25 mixtures specifically reduced the expression of miR-18, miR-19 and miR-25 family members, respectively, without affecting the expression of unrelated miRNAs (Fig. 2B–D and Supplementary Fig. 1 and 2). To further rule out cross reactivity, we analyzed the expression of miR-21, an abundantly expressed, pathogenic miRNA in PKD[8,11,14,25]. miR-21 levels did not change in kidneys from mice treated with PBS compared to kidneys from mice treated with either anti-miR-17, 18, 19, or 25 mixtures (Fig. 2E). A heat map summarizing these results is shown in Fig. 2F. These results indicate that anti-miRs specifically target the cognate miRNA family members without affecting the expression of unrelated miRNAs.

Anti-miR-17, but not anti-miR-18, anti-miR-19 or anti-miR-25, attenuates cyst growth. To determine the effects of individually inhibiting each miRNA family on ADPKD progression, we evaluated cyst burden in mice treated with anti-miRs compared to PBS. Kidney histology was improved in anti-miR-17 treated

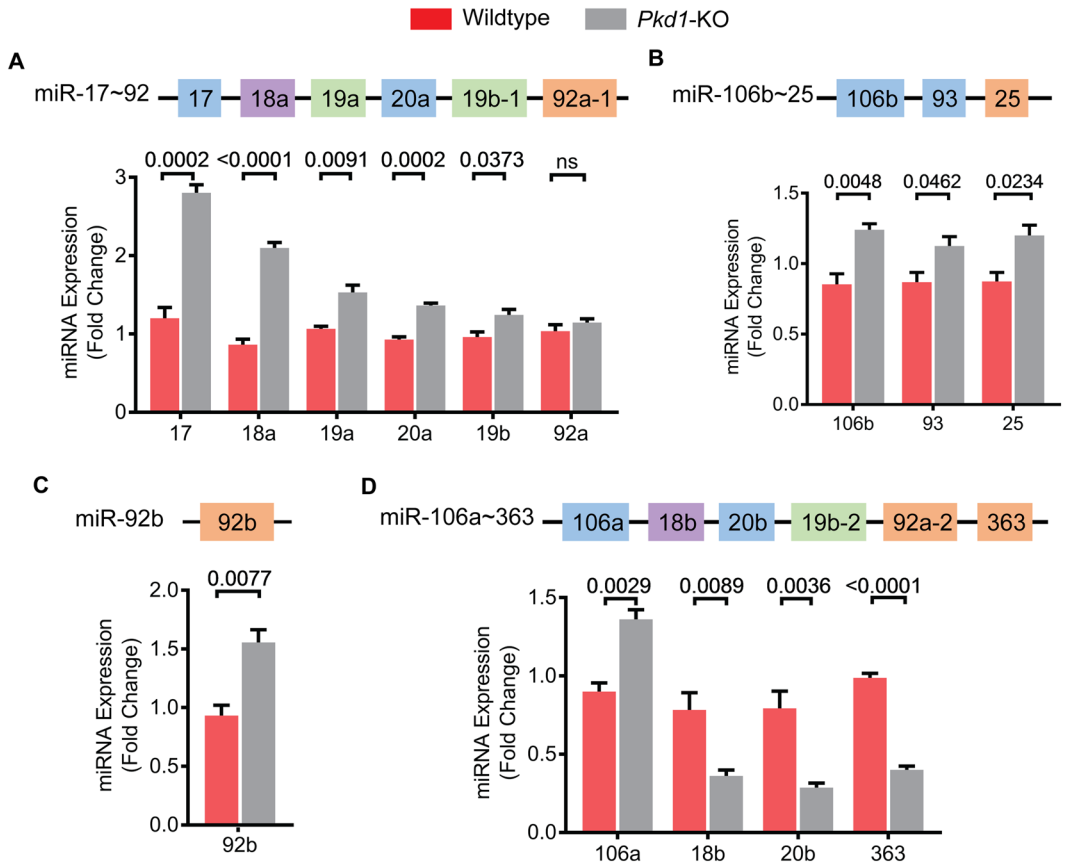

Figure 1. Expression of miR-17~92 and related clusters in *Pkd1*-KO kidneys. The miR-17~92, miR-106a~363, miR-106b~25, and miR-92b encode miRNAs belonging to four families: miR-17 (blue), miR-18 (purple), miR-19 (green), and miR-25 (orange). miRNAs are color-coded based on their family. (**A**–**C**) Q-PCR analysis showed that the expression of five of the six miRNAs derived from the miR-17~92 cluster, all three miRNAs derived from the miR-106b~25 cluster, and the independently transcribed miR-92b are upregulated in *Pkd1*-KO compared to control kidneys. (**D**) miRNAs derived from the miR-106a~363 cluster showed variable expression. miR-106a expression was increased whereas miR-18b, 20b, and miR-363 expression was decreased. Wildtype n = 3, *Pkd1*-KO n = 5. All mice were 3 weeks of age. Data are presented as mean ± SEM. Statistical analyses: Student's t-test, ns indicates $P > 0.05$.

mice, but not in mice treated with anti-miR-18, anti-miR-19, or anti-miR-25 (Fig. 3A). No significant differences in body weight were found during any point in this study between treated and untreated mice (Supplementary Fig. 2). However, kidney-weight-to-body-weight ratio (KW/BW) was reduced by 30.5% in mice treated with anti-miR-17 mixtures compared to PBS. In contrast, KW/BW ratio was not reduced in mice treated with anti-miR-18, anti-miR-19, or anti-miR-25 (Fig. 3B). In fact, anti-miR-19 family treatment increased KW/BW by 31.4%. Moreover, cyst-index was reduced by 35.2% in anti-miR-17-treated mice compared to PBS-treated mice, but no change in cyst index was observed in mice treated with anti-miR-18, anti-miR-19, or anti-miR-25 mixtures (Fig. 3C). H&E of kidneys from all mice is shown in Supplementary Fig. 3. To assess renal function, we measured blood urea nitrogen (BUN) levels, which was reduced by 23% in mice treated with anti-miR-17 compared to PBS (Fig. 4A). However, this observation did not reach statistical significance. No improvement in BUN was observed in mice treated with other anti-miRs mixtures. Phenotypic data of all mice analyzed in this study are shown in Supplementary Table 2.

Anti-miR-17 also reduced kidney injury assessed by measuring the expression of kidney injury markers, *Kim1* and *Ngal*. Q-PCR analysis revealed a 55.1% reduction in *Kim1* and a 44.1% reduction in *Ngal* only in anti-miR-17 treated mice (Fig. 4B,C). Next, we determined whether anti-miR-17 affected cyst proliferation. The number of cyst epithelial cells expressing phospho-histone H3, a marker of mitosis, was reduced by 44.6% in anti-miR-17 treated compared to PBS treated mice (Fig. 4D,E). No change in cyst proliferation was observed in other groups. Thus, our results indicate that treatment with anti-miR-17, but not anti-miR-18, anti-miR-19, or anti-miR-25 mixtures, reduced cyst progression and improved kidney function. These results suggest that within miR-17~92 and related clusters, the miR-17 family is the pathogenic element and the primary contributor to cyst progression.

Anti-miR-17 treatment recapitulates the gene expression pattern observed after miR-17~92 deletion in *Pkd1*-KO kidneys. To understand the mechanism by which anti-miR-17 mediates its cyst-reducing effects, we began by performing RNA-seq analysis to compare gene expression profiles between

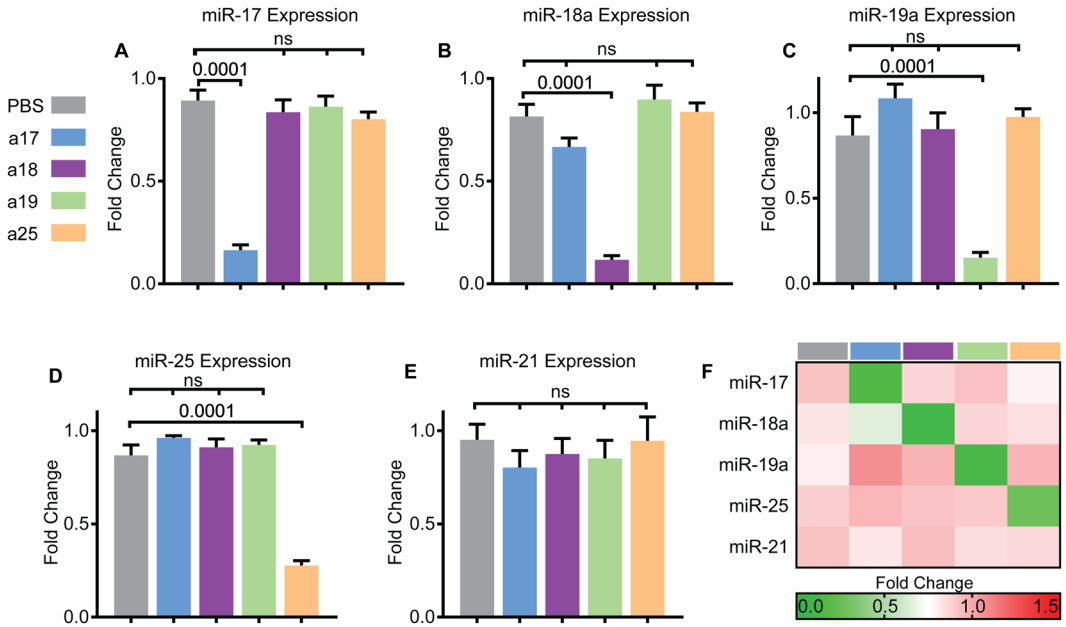

Figure 2. Anti-miR mixtures specifically inhibit cognate miRNAs. *Pkd1*-KO mice were randomized to receive PBS, anti-miR-17 (a17), anti-miR-18 (a18), anti-miR-19 (a19), or anti-miR-25 (a25) family inhibitors. (**A**) Q-PCR analysis revealed that the expression of miR-17 is reduced only in mice treated with anti-miR-17 but not in mice treated with anti-miRs against other families. (**B**–**D**) Similarly, miR-18, miR-19, and miR-25 levels are reduced only in mice treated with the respective anti-miRs. (**E**) Q-PCR analysis showed that anti-miR treatment did not affect the levels of miR-21, an abundantly expressed pathogenic miRNA in ADPKD, further demonstrating no off-target effects. (**F**) Heat map summary of Q-PCR data is shown. Data are presented as mean ± SEM, n = 8 per group. Statistical analyses: One-way ANOVA (post hoc analysis: Dunnett's multiple comparisons test), ns indicates $P > 0.05$.

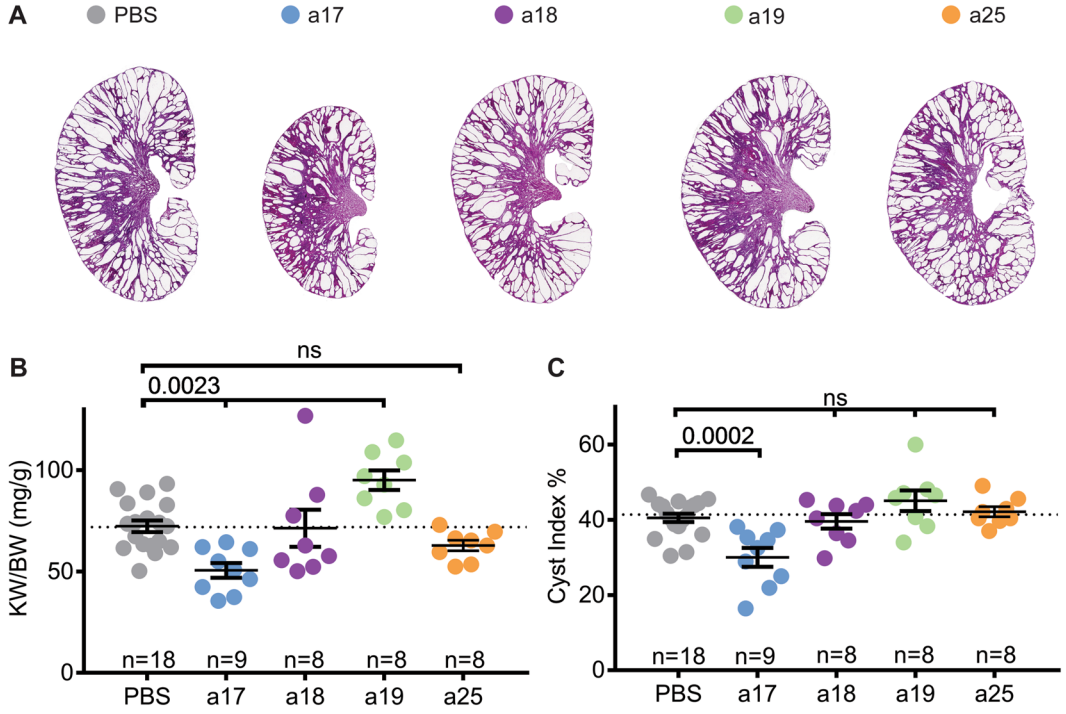

Figure 3. Anti-miR-17 but not anti-miR-18, anti-miR-19, or anti-miR-25 reduced cyst progression. (**A**) Representative H&E-stained kidney sections from *Pkd1*-KO mice treated anti-miR-17 (a17), anti-miR-18 (a18), anti-miR-19 (a19), or anti-miR-25 (a25) mice are shown. Only mice treated with anti-miR-17 showed reduction in kidney size. (**B**) Kidney-weight-to-body weight ratios (KW/BW) and (**C**) cyst index were reduced only in mice treated with anti-miR-17 treated mice compared to PBS. Data are presented as mean ± SEM. Statistical analyses: One-way ANOVA (post hoc analysis: Dunnett's multiple comparisons test), ns indicates $P > 0.05$.

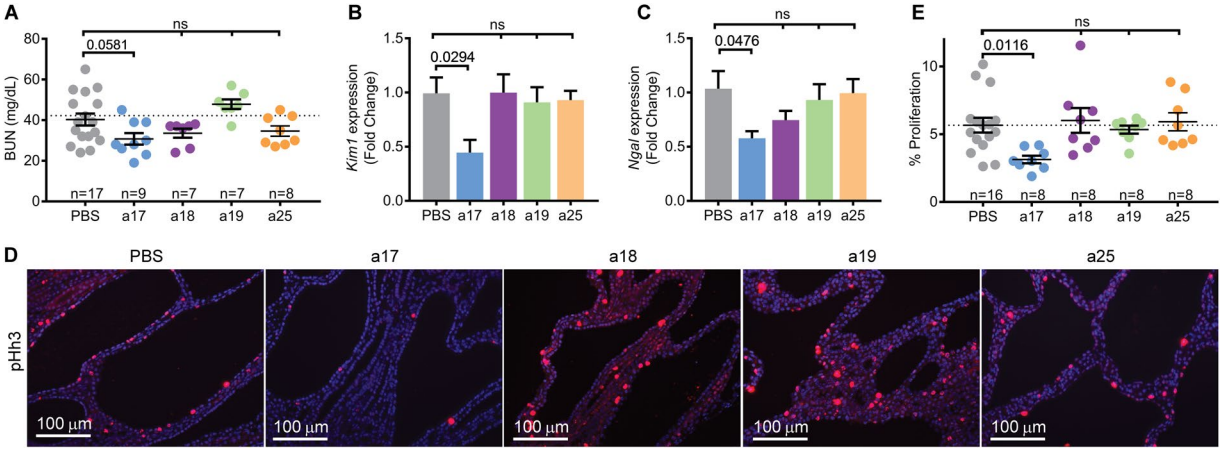

Figure 4. Anti-miR-17 improves renal function and reduces kidney injury and cyst proliferation. (**A**) Blood urea nitrogen (BUN) was decreased by 23% in anti-miR-17 treated mice compared to PBS treated mice. However this difference was not statistically significant. (**B**,**C**) Q-PCR analysis revealed that expression of kidney injury markers, *Kim1* and *Ngal* was also reduced only in kidneys of anti-miR-17-treated mice. (N = 6 per group) (**D**,**E**) To assess proliferation, kidney sections were stained using an antibody against phosphohistone-H3 (pHh3), a marker of proliferating cells. Quantification of PHh3 positive cells from ten random high-powered images (20×) from each kidney section revealed that only anti-miR-17-treated mice showed a reduction in the number of proliferating cyst cells. Data are presented as mean ± SEM. Statistical analyses: One-way ANOVA (post hoc analysis: Dunnett's multiple comparisons test), ns indicates $P > 0.05$.

kidneys of anti-miR-17 treated mice and PBS treated mice (n = 3, each group). Pathway analysis of the differentially expressed genes revealed that the primary consequence of anti-miR-17 treatment was upregulation of mitochondrial metabolism pathways (oxidative phosphorylation (OXPHOS), mitochondrial function, fatty acid oxidation (FAO)) and downregulation of the inflammation and fibrosis pathways (atherosclerosis signaling, granulocyte adhesion, acute response signaling, etc.) (Fig. 5A). Ingenuity pathway analysis software was used to identify the upstream regulators (URs) that could be responsible for the gene expression changes observed after anti-miR-17 treatment. This analysis showed that mitochondrial and metabolism-related gene networks regulated by *Ppara*, *Pparg*, *Ppard*, and others were activated. In contrast, inflammation-associated gene networks were inhibited including those controlled by *Il1b* and *Tnf*. We have previously performed RNA-Seq analysis and identified genes that are differentially expressed as a result of miR-17~92 genetic deletion in *Pkd1*-KO kidney[15]. We intersected the two RNA-seq datasets to discover a common gene signature between the genetic (miR-17~92 deletion) and pharmaceutical (anti-miR-17 treatment) approaches. There were 292 common differentially expressed genes found in both datasets. Unbiased One-minus Pearson hierarchal clustering using these 292 genes segregated the samples into two groups. *Pkd1*-KO kidneys without miR-17~92 deletion and PBS-treated *Pkd1*-KO kidneys clustered as one group whereas *Pkd1*-miR-17~92 double knockout kidneys and anti-miR-17 treated *Pkd1*-KO kidneys segregated as the second group. Pathway analysis using the 292 common genes also showed activation of mitochondrial function/metabolism and inhibition of inflammation (Fig. 5E). Moreover, URs *Ppara* and *Pparg* were predicted to be activated whereas inflammation-associated gene networks regulated by *Il1b, Tnf*, and other were predicted to be inhibited. Collectively, these results indicate that inhibition of the miR-17 family largely recapitulates the gene expression patterns observed due to miR-17~92 deletion in *Pkd1*-KO kidneys.

Anti-miR-17 normalized kidney metabolism and reduced inflammation. Based on the unbiased analysis of our RNA-Seq data, we reasoned that anti-miR-17 treatment attenuates cyst growth by improving cyst metabolism and inhibiting cyst-associated inflammation. We also analyzed kidneys of mice treated with anti-miR-18 to test whether the molecular effects were specific to anti-miR-17 treatment. Q-PCR analysis revealed reduced expression of miR-17 targets *Ppara* (down by 68%) and *Ppargc1a* (down by 48%) in PBS-treated *Pkd1*-KO kidneys compared to wild-type control kidneys. *Ppara* and *Ppargc1a* expression was increased by 61% and 51%, respectively, in anti-miR-17-treated compared to PBS-treated *Pkd1*-KO kidneys (Fig. 6A). In contrast, *Ppara* and *Ppargc1a* expression was not different between PBS and anti-miR-18-treated kidneys. Thus, upregulation of these key transcription factors that regulate a network of mitochondrial metabolism-related genes was specifically observed only after anti-miR-17 treatment[26–29]. To determine if the electron transport chain (ETC) components were increased, we analyzed the expression of genes encoding subunits of each complex in the ETC (Fig. 6A). *Ndufv1* (NADH dehydrogenase flavoprotein 1) and *Ndufa2* (NADH dehydrogenase 1 alpha subcomplex subunit 2) are both found in complex I[30,31]. Their expression was reduced in PBS-treated *Pkd1*-KO kidneys compared to non-cystic control kidneys. Anti-miR-18 treatment had no effect, but anti-miR-17 treatment restored their expression to wild-type levels. Similarly, the expression of *Ppara* target gene *Etfa* (Electron Transfer Flavoprotein Alpha) found in complex II[32], was reduced in PBS-treated *Pkd1*-KO kidneys compared to non-cystic control kidney but was it restored to near wild-type levels after anti-miR-17 treatment. Expression of *Cox5a* (Cytochrome c oxidase subunit 5a) found in complex IV[33] and *Atp5e* that encodes a subunit of ATP synthase in

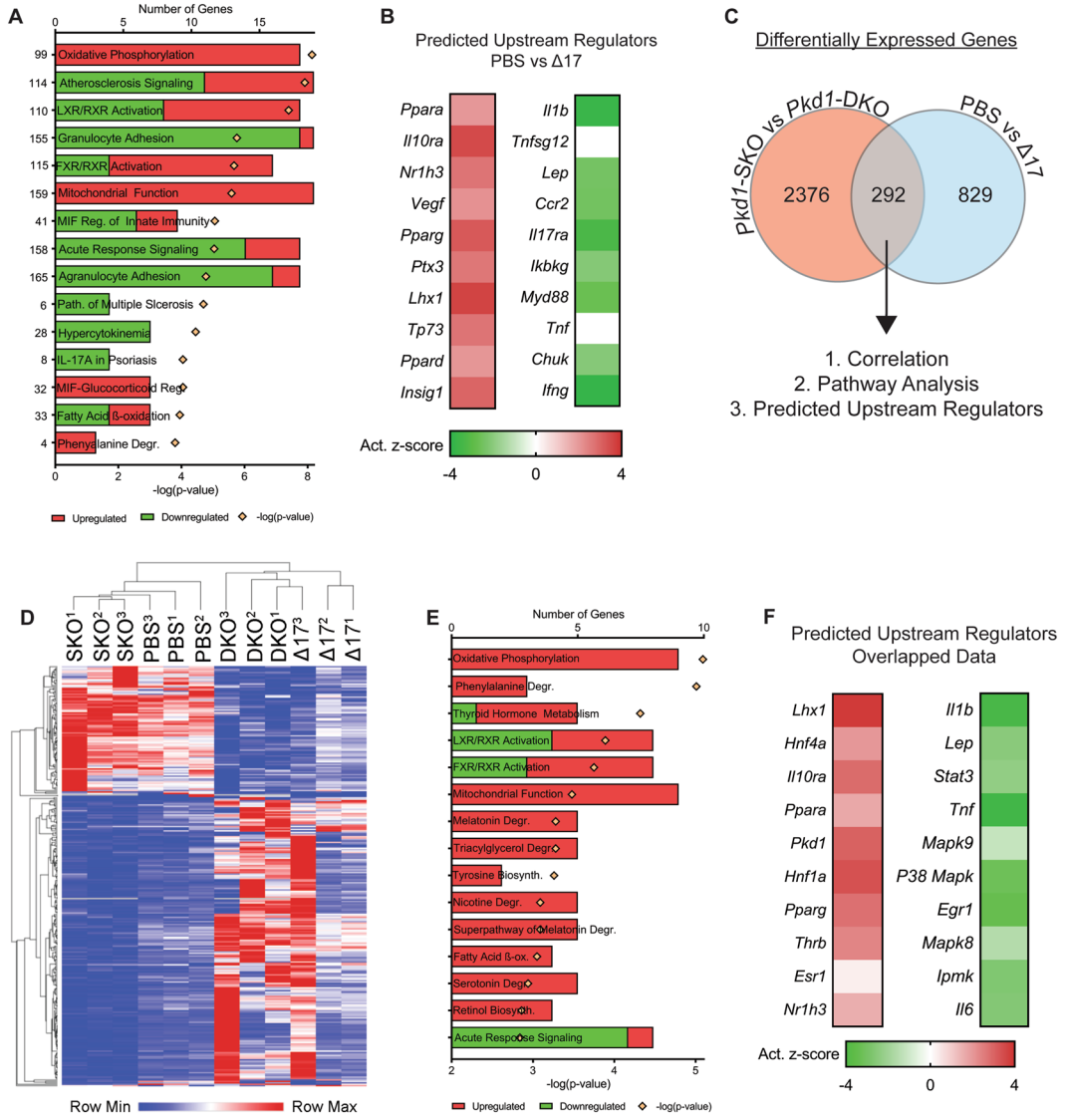

Figure 5. Anti-miR-17 treatment recapitulates the gene expression pattern observed after miR-17~92 deletion. RNA-seq analysis was performed using kidney RNA from PBS-treated and anti-miR-17-treated mice (a17) (n = 3). (**A**) The top differentially regulated pathways in anti-miR-17-treated mice compared to PBS-treated mice are shown. Red indicates activation and green indicates inhibition of the indicated pathways (**B**) Ingenuity pathway analysis software was used to identify upstream regulators (URs) that may underlie the changes observed in gene expression. The activation z-scores of the top 10 most significantly upregulated (orange) and downregulated URs (blue) are shown. Positive z-scores (orange) indicate activation whereas negative z-scores (blue) indicate inhibition. (**C**) To determine if there is a common gene signature underlying the reduction in cyst growth observed between the anti-miR-17 and miR-17~92 genetic deletion, previous RNA-seq data (NCBI repository accession number GSE89764) comparing *Pkd1*$^{F/RC}$ (*Pkd1*-SKO) and *Pkd1*;$^{F/RC}$ miR-17~92-KO (*Pkd1*-DKO) was intersected with the current data. There were 292 common, differentially regulated genes between the two data sets. (**D**) Unbiased hierarchical clustering of these 292 genes is shown. *Pkd1*-SKO and PBS-treated *Pkd1*-KO kidneys clustered as one group whereas *Pkd1*-DKO and anti-miR-17-treated *Pkd1*-KO kidneys clustered together as a second independent group. (**E**,**F**) Pathways and UR analysis of the common gene signature (obtained from analysis in C) also revealed an increase in mitochondrial metabolism and reduction in inflammation.

complex V[34] was also increased after anti-miR-17 treatment. Again, anti-miR-18 treatment did not affect *Etfa*, *Cox5a*, or *Atp5e* expression indicating an effect that was specific to anti-miR-17 treatment.

To further characterize the metabolic phenotype of anti-miR-17 treated mice, we analyzed proteins in the mTOR pathway. This pathway is well known to regulate both glycolysis and mitochondrial metabolism[35–37], and could partially explain the improvement of metabolism in anti-miR-17 treated mice. Western blot analysis revealed that both the active and total mTOR (Fig. 6B) levels are increased in PBS-treated *Pkd1*-KO kidneys compared to non-cystic control kidneys. Treatment with anti-miR-17, but not with anti-miR-18, reduced active and total mTOR levels. Moreover, the expression of phosphorylated forms of p70S6K and 4EBP1 were also

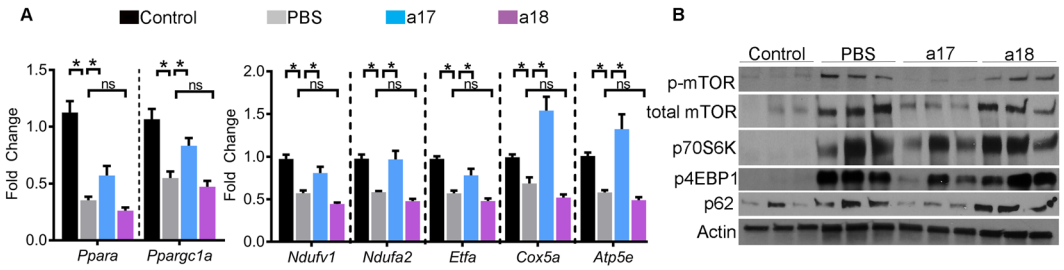

Figure 6. Anti-miR-17 upregulated metabolism-related genes and suppressed mTOR pathway. (**A**) Q-PCR analysis revealed that the expression mitochondrial metabolism-related genes is downregulated in PBS-treated *Pkd1*-KO kidneys compared to control (non-cystic) kidneys. Anti-miR-17 treatment increased the expression of these genes compared to PBS-treated kidneys whereas anti-miR-18 treatment had no effect. N = 5 per group. (**B**) Western Blot analysis showed that the mTOR pathway is upregulated and cellular autophagy is reduced in PBS-treated *Pkd1*-KO kidneys compared to control (non-cystic) kidneys. Anti-miR-17 treatment, but not anti-miR-18 treatment, inhibited the mTOR pathway and induced autophagy. Data are presented as mean ± SEM. Statistical analyses: Student's t-test, ns indicates $P > 0.05$.

significantly decreased only after anti-miR-17 treatment. Defective autophagy is observed in ADPKD models[38]. Inhibition of the mTOR pathway and improving cyst-metabolism has been shown to induce autophagy[39]. Consistent with these observations, western blot analysis revealed downregulation of P62 suggesting an increase in autophagy in anti-miR-17-treated kidneys compared to PBS-treated kidneys. This effect was not observed after anti-miR-18 treatment.

Based on the RNA-Seq data, we next validated whether the inflammatory pathways were downregulated in anti-miR-17-treated mice. Q-PCR analysis revealed that the expression of *Acta2* and *Col1a1*, two markers of fibrosis, is markedly increased in *Pkd1*-KO kidneys compared to control kidneys. Anti-miR-17 treatment reduced *Acta2* and *Col1a1* expression by 25% and 35%, respectively (Fig. 7A). In contrast, anti-miR-18 treatment had no effect. Expression of cytokines *Tgfb2*, *Ifng*, *Ccl5*, *Ccl22*, *Il6*, and *Mip2* was also increased in *Pkd1*-KO kidneys compared to control kidneys. Anti-miR-17 treatment reduced their expression by 30%, 47%, 50%, 53%, 27%, and 34.9%, respectively, compared to PBS-treated kidneys (Fig. 7B). Macrophages surrounding cysts consist of a heterozygous population of M1-like and M2-like macrophages, with the latter of the two thought to promote cyst growth[40,41]. Accordingly, Q-PCR analysis showed that the markers of the pathogenic M2-like macrophages, *Arg1* and *Mrc1*, were upregulated in *Pkd1*-KO kidneys compared to control kidneys. Moreover, western blot analysis and immunohistochemistry analysis also showed increased MRC1 expression in *Pkd1*-KO kidneys compared to control kidneys (Fig. 7C,D). In comparison to PBS treatment, anti-miR-17 treatment reduced *Arg1* and MRC1 expression. Expression of *Tgfb2* and *Il6* was unchanged, but the expression other inflammatory marker genes was reduced in anti-miR-18-treated kidneys compared to PBS-treated kidneys suggesting that anti-miR-18 treatment may have a partial anti-inflammatory effect.

Discussion

The first new insight from our studies is that, within the miR-17~92 microRNA cluster, the miR-17 family is the primary pathogenic component that promotes ADPKD progression. We have previously shown that genetic inactivation of the miR-17~92 cluster attenuates disease progression in multiple ADPKD animal models[15]. Thus, this cluster has emerged as a novel therapeutic target for ADPKD. However, the genetic approach reduced the expression of all miRNAs encoded by miR-17~92 precluding analysis of the individual pathogenic contributions of these miRNAs. Therefore, miRNAs within this cluster that should be therapeutically targeted have thus far remained unknown. We performed an *in-vivo* anti-miR screen to individually inhibit either miR-17, miR-18, miR-19, or miR-25 families in an orthologous mouse model of ADPKD. Treatment with anti-miR-17 family inhibitors recapitulated the anti-proliferative, cyst-reducing effects of deleting the entire miR-17~92 cluster. In contrast, inhibiting miR-18, miR-19, or miR-25 families had no impact on cyst growth. Hence, our results argue against functional cooperation between the various families in promoting cyst growth and instead point to the miR-17 family as the primary driver of PKD pathogenesis. These results suggest that rather than a complicated drug discovery process to inhibit different families within the miR-17~92 cluster simultaneously, a more simplified approach focused on targeting the miR-17 family alone will be sufficient in ADPKD. Our results provide a clear stepping stone for developing pharmaceutical grade anti-miRs against the miR-17 family.

miR-17~92 gene produces a single transcript, which gives rise to six individual mature miRNAs[23]. However, the six miRNAs are processed with varying efficiencies producing different amounts of mature miRNAs[42,43]. Consistent with this notion, even though the miR-17~92 gene is transcriptionally activated in ADPKD, the final level of mature miR-17 upregulation is much more pronounced than other miRNAs derived from this transcript. In fact, the miR-17 family alone accounts for more than 2.7% to the total dysregulated pool of all miRNAs, not just those produced by miR-17~92[15]. In contrast, other miR-17~92 cluster families have minimal or no impact to the dysregulated miRNA pool in ADPKD models. This outsized contribution to the pathogenic miRNA pool may provide one explanation for why the miR-17 family appears to be the sole driver of cyst growth within the miR-17~92 cluster. Similar observations of specialization among members of this cluster have been made in other studies. Feingold syndrome, a genetic disease primarily characterized by short stature and skeletal abnormalities, can be caused due to germline microdeletions involving miR-17~92[44]. The deletion of miR-17 seed family is

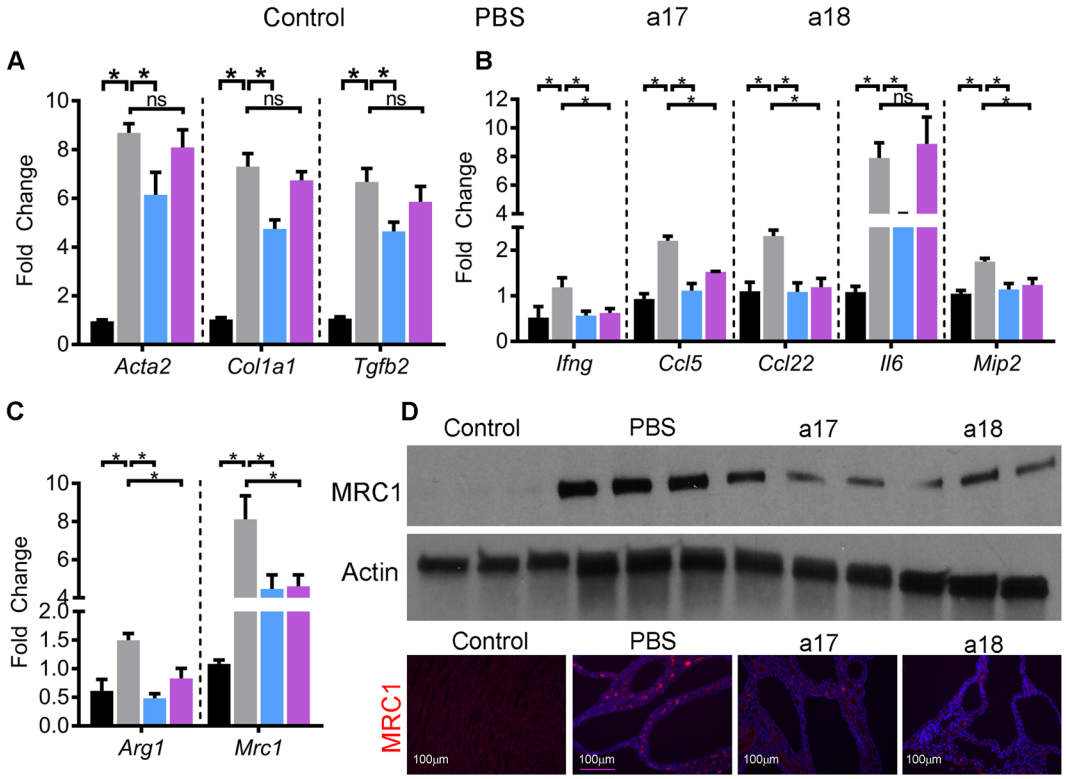

Figure 7. Anti-miR-17 treatment reduced fibrosis, inflammation, and M2-like macrophages. (**A,B**) Q-PCR analysis demonstrated that the expression of fibrosis and inflammation-related genes is markedly increased in PBS-treated *Pkd1*-KO kidneys compared to control (non-cystic) kidneys. Expression of these genes was reduced in anti-miR-17-treated kidneys compared to PBS-treated kidneys. Anti-miR-18 treatment did not affect the expression of fibrosis-related genes but reduced the expression many inflammation-related genes (N = 5 per group). (**C**) Q-PCR analysis of M2-like macrophage markers *Arg1* and *Mrc1* in the indicated groups is shown. (**D**) Western blot and immunofluorescence analysis revealed that MRC1 expression was increased in PBS-treated *Pkd1*-KO compared to control (non-cystic) kidneys. Both anti-miR-17 and anti-miR-18 treatment reduced MRC1 expression. Data are presented as mean ± SEM. Statistical analyses: Student's t-test, ns indicates $P > 0.05$.

sufficient to reproduce the skeletal malformations observed in Feingold syndrome, whereas individually deleting the other seed families has no effect. Similarly, the miR-17~92 cluster is essential for early B-cell development, and miR17/18 seed families appear to be solely responsible for this effect[45]. Finally, the miR-17~92 cluster is amplified and oncogenic in lymphoma, and miR-19 overexpression is sufficient to reproduce this oncogenicity fully[46]. Interestingly, despite this well-described role of miR-19 in promoting proliferation and cancer growth, we found that in the context of ADPKD, it does not have a significant pathogenic affect.

The second new insight from our work is that the beneficial effects of anti-miR-17 treatment are due to the regulation of multiple cyst-promoting, pathogenic pathways (mitochondrial metabolism, mTOR pathway, and inflammation). Consistent with our earlier observations, the primary cellular consequence of anti-miR-17 treatment was improved expression of metabolism-related gene networks, including the upregulation of direct miR-17 target *Pparα* and *Ppargc1a*. Thus, one of the direct mechanisms by which anti-miR-17 mediates its cyst-reducing effects may be through improvement in cyst metabolism. We have recently shown that PPARA upregulation is sufficient to improve cyst metabolism and attenuate cyst growth[26]. Hence, stabilizing *Pparα* mRNA transcript could be a complementary or an alternative therapeutic approach for ADPKD. Our results also suggest that non-invasive assessment of various metabolic parameters could serve as potential pharmacodynamic biomarkers that predict anti-miR-17 function. As new mechanistic insights, we demonstrate that anti-miR-17 treatment inhibits mTOR signaling, which is intimately linked to the metabolic state of the cell. Activation of mTOR signaling has been linked to PKD pathogenesis. Our results suggest that, in addition to improving cyst metabolism, anti-miR-17 therapy could potentially alleviate cyst growth via regulation of the mTOR pathway. We found that another consequence of anti-miR-17 treatment is the inhibition of various inflammation-related gene networks. We extended this observation and found that anti-miR-17 reduced cyst-associated macrophages particularly the M2-like macrophages, which have been shown to promote cyst growth[40]. Whether the inhibition of mTOR signaling and inflammation is a direct or indirect effect of anti-miR-17 treatment remains unknown.

Several questions have remained unanswered. The purpose of this screen was to uncover the pathogenic components within the miR-17~92 cluster in the context of ADPKD. Therefore, we elected to perform a short-term (five day), *in-vivo* screen directed at miR-17~92 and related clusters. Whether sustained inhibition of miR-17 family would produce a long-term beneficial effect was not addressed. Additionally, whether sustained miR-17

inhibition is safe and efficacious over the long term was also not studied. In our previous study, we genetically deleted the miR-17~92 cluster in the *Pkd1*-KO mice. miR-17~92 deletion essentially restored normal life span in *Pkd1*-KO mice. Moreover, in that study, long-term (~6-months) treatment of *Nphp3*$^{pcy/pcy}$ mice, a slow growth cystic disease model, with an anti-miR-17 compound also demonstrated a sustained benefit in attenuating cyst growth. Thus, our work suggests that sustained miR-17 inhibition is safe. A second limitation is that we performed this study in only one model of ADPKD. We chose the *Pkd1*-KO mouse model because the majority of patients with ADPKD have a mutation in the *PKD1* gene. Furthermore, anti-miR treatment has never been performed in a *Pkd1*-KO model. Nevertheless, we have previously shown that genetic knockout of miR-17~92 or pharmaceutical inhibition of miR-17 both reduce cyst burden in an orthologous *Pkd2*-KO mouse model. Therefore, the miR-17 family is also likely to be the primary driver of PKD pathogenesis in *Pkd2*-KO mice. Lastly, we did not study synergism between the various miR-17~92 cluster families. We also have not genetically deleted miR-106a~363 and 106b~25 clusters in ADPKD models. These miRNA clusters/families have many overlapping mRNA targets. Perhaps co-inhibition of two or more miRNA families could have an additive effect.

In summary, our studies suggest that the pathogenic component of the miR-17~92 cluster lies within the miR-17 family. Moreover, inhibition of only the miR-17 family recapitulated the mechanistic effects of miR-17~92 genetic deletion. Thus, our study provides a strong rationale for developing drugs against the miR-17 seed in ADPKD.

Materials and Methods

Mice. KspCre/*Pkd1*$^{F/RC}$ mice were used for these studies. At 10 days of age KspCre/*Pkd1*$^{F/RC}$ mice were randomized to receive PBS, Anti-miR-17 family cocktail, Anti-miR-18 family cocktail, Anti-miR-19 family cocktail, and Anti-miR-25 family cocktail (20 mg/kg total). Based on our previous experience, power analysis (alpha $<$5% and power $>$80%) was performed *a priori* to determine the sample size (n of at least 8). Mice were given intraperitoneal injections at postnatal day (P) 10, 11, 12, and 15, and were sacrificed at P18. All experiments involving animals were approved by the UTSW Animal Care and Use Committee. All experiments were performed in accordance with Institutional Animal Care and Use Committee guidelines and regulations. Equal males and females were used in all groups for all studies.

Anti-miRs. Anti-miRs were acquired from Exiqon (Denmark). *In vivo* grade locked nucleic acid-modified anti-miRs were used. Each anti-miR was dissolved in PBS to create a 2 mg/uL stock which was kept at −20 °C. On the day of injection, each anti-miR was thawed to 4 °C and added to its respective anti-miR cocktail. A total dose of 20 mg/kg for each cocktail was injected. See Supplementary Table 1 for individual inhibitor product number, sequence, and target information.

Tissue harvesting and analysis. Mice were anesthetized under approved protocols, blood was obtained via cardiac puncture. The right kidney was flash frozen for molecular analysis, and the left kidney was perfused with cold PBS and 4% (wt/vol) paraformaldehyde and then harvested. Kidneys were fixed with 4% paraformaldehyde for 2 hours and then embedded in paraffin for sectioning. Sagittal sections of kidneys were stained with hematoxylin and eosin (H&E) for cyst index analysis using Image J software.

Renal function tests. BUN was measured using the Vitros 250 Analyzer.

RNA Isolation and quantitative RT-PCR (Q-PCR). Total RNA was isolated from mouse kidneys using miRNeasy Mini kits (Qiagen). First-strand cDNA was synthesized from mRNA using the iScript cDNA synthesis kit (Bio-Rad) and Superscript III (Invitrogen), and Q-PCR was performed using the iQ SYBR Green Supermix (Bio-Rad). The Universal cDNA Synthesis kit from Exiqon was used for first-strand synthesis from miRNA. Q-PCR was performed by using miRNA-specific forward and reverse locked nucleic acid (LNA)-enhanced PCR primers from Exiqon. The samples were loaded in duplicate on a CFX ConnectTM Real-time PCR detection system. 18S and SNORD68 RNA were used to normalize expression of mRNA and miRNA, respectively. Data were analyzed using the Bio-Rad CFX software. The sequences of the PCR primers are shown in Supplementary Table 2.

RNA sequencing. Total RNA was extracted from whole kidney lysate of three PBS treated and anti-miR-17 treated mice. Strand specific RNA-Seq libraries were prepared using the TruSeq Stranded Total RNA LT Sample Prep Kit from Illumina. After quality check and quantification, libraries were sequenced at the UT Southwestern McDermott Center using a Hiseq. 2500 sequencer to generate 51 bp single-end reads. Before mapping, reads were trimmed to remove low quality regions in the ends. Trimmed reads were mapped to the mouse genome (mm10) using TopHat v2.0.12 with the UCSC iGenomes GTF file from Illumina. Alignments with mapping quality less than 10 were discarded. Expression abundance estimation and differential expression gene identification were done using edgeR. Genes with a P-value < 0.05 were deemed significantly differentially expressed between the two conditions.

Immunofluorescence staining. The following antibodies and dilutions were used on paraffin embedded section for immunofluorescence staining: phosphohistone H3 (1:400, Sigma-Aldrich H0412), and anti-Mannose Receptor (Abcam ab64693, 1:400). Secondary antibodies were conjugated to Alexa Fluor 594 (Molecular Probes, 1:400).

Immunofluorescence quantification. Image J's Find Maxima feature was utilized to determine the percentage of phospho-histone H3 or MRC1 positive cells from ten random high powered (20×) fields from

each kidney section. An average of 6300 cells were counted per mouse. The total number of mice analyzed for phospho-histone H3 or MRC1 quantification are shown in Figs 4 and 7, respectively.

Western blot analysis. Total protein was extracted from kidneys. 15 µg of protein was loaded on a 4–20% SDS-polyacrylamide gel, and the proteins were transferred to a nitrocellulose membrane. The membrane was blocked with 5% milk and probed overnight at 4 °C with antibodies (Dilution 1:1000): ATP5e (Abcam ab110413), pmTOR (Cell Signaling #2971), Total mTOR (Cell Signaling #2972), p4EBP1(Cell Signaling #2855), pS6RP (Cell Signaling #2211), and Mannose Receptor 1 (Abcam ab64693). Goat-anti-rabbit HRP-conjugated IgG was used as the secondary antibody. The blot was developed using the SuperSignal West Dura Extended Duration substrate from Pierce. The protein bands were quantified using Quantity One imaging software from Bio-Rad.

Clustering analysis. Heat map and clustering analysis was performed using Morpheus software found at: https://software.broadinstitute.org/morpheus/

Statistical analysis. Statistical analysis was performed using One-way ANOVA. Next, a post hoc analysis (Dunnett's one way multiple comparisons test) was performed using PBS as the control group. P-values indicate significant differences between PBS treatment and respective anti-miR treatment. Lastly, Student's *t*- test was performed in analyses with two groups. Data are shown as the mean ± SEM.

References

1. Igarashi, P. & Somlo, S. Polycystic kidney disease. *Journal of the American Society of Nephrology* **18**, 1371–1373 (2007).
2. Patel, V., Chowdhury, R. & Igarashi, P. Advances in the pathogenesis and treatment of polycystic kidney disease. *Current opinion in nephrology and hypertension* **18**, 99 (2009).
3. Harris, P. C. & Torres, V. E. Polycystic kidney disease. *Annual review of medicine* **60**, 321–337 (2009).
4. Bartel, D. P. MicroRNAs: genomics, biogenesis, mechanism, and function. *cell* **116**, 281–297 (2004).
5. Bartel, D. P. MicroRNAs: target recognition and regulatory functions. *cell* **136**, 215–233 (2009).
6. Pereira, D. M., Rodrigues, P. M., Borralho, P. M. & Rodrigues, C. M. Delivering the promise of miRNA cancer therapeutics. *Drug discovery today* **18**, 282–289 (2013).
7. Hayashita, Y. *et al*. A polycistronic microRNA cluster, miR-17-92, is overexpressed in human lung cancers and enhances cell proliferation. *Cancer research* **65**, 9628–9632 (2005).
8. Asangani, I. A. *et al*. MicroRNA-21 (miR-21) post-transcriptionally downregulates tumor suppressor Pdcd4 and stimulates invasion, intravasation and metastasis in colorectal cancer. *Oncogene* **27**, 2128 (2008).
9. Burk, U. *et al*. A reciprocal repression between ZEB1 and members of the miR-200 family promotes EMT and invasion in cancer cells. *EMBO reports* **9**, 582–589 (2008).
10. Patel, V. *et al*. miR-17~92 miRNA cluster promotes kidney cyst growth in polycystic kidney disease. *Proceedings of the National Academy of Sciences* **110**, 10765–10770 (2013).
11. Lakhia, R. *et al*. MicroRNA-21 aggravates cyst growth in a model of polycystic kidney disease. *Journal of the American Society of Nephrology* **27**, 2319–2330 (2016).
12. Gomez, I. G. *et al*. Anti–microRNA-21 oligonucleotides prevent Alport nephropathy progression by stimulating metabolic pathways. *The Journal of clinical investigation* **125**, 141–156 (2015).
13. Obad, S. *et al*. Silencing of microRNA families by seed-targeting tiny LNAs. *Nature genetics* **43**, 371 (2011).
14. Yheskel, M. & Patel, V. Therapeutic microRNAs in polycystic kidney disease. *Current opinion in nephrology and hypertension* **26**, 282–289 (2017).
15. Hajarnis *et al*. microRNA-17 family promotes polycystic kidney disease progression through modulation of mitochondrial metabolism. *Nature communications* **8**, 14395 (2017).
16. Huang, X. *et al*. Lipid Nanoparticle–Mediated Delivery of Anti-miR-17 Family Oligonucleotide Suppresses Hepatocellular Carcinoma Growth. *Molecular cancer therapeutics* **16**, 905–913 (2017).
17. Dhanasekaran, R. *et al*. Anti-miR-17 therapy delays tumorigenesis in MYC-driven hepatocellular carcinoma (HCC). *Oncotarget* **9**, 5517 (2018).
18. Murphy, B. L. *et al*. Silencing of the miR-17~92 cluster family inhibits medulloblastoma progression. *Cancer research* **73**, 7068–7078 (2013).
19. Molitoris, J. K., McColl, K. S. & Distelhorst, C. W. Glucocorticoid-mediated repression of the oncogenic microRNA cluster miR-17~92 contributes to the induction of Bim and initiation of apoptosis. *Molecular Endocrinology* **25**, 409–420 (2011).
20. Badal, S. S. & Danesh, F. R. MicroRNAs and their applications in kidney diseases. *Pediatric nephrology* **30**, 727–740 (2015).
21. Matsubara, H. *et al*. Apoptosis induction by antisense oligonucleotides against miR-17-5p and miR-20a in lung cancers overexpressing miR-17-92. *Oncogene* **26**, 6099 (2007).
22. Nowakowski, T. J. *et al*. MicroRNA-92b regulates the development of intermediate cortical progenitors in embryonic mouse brain. *Proceedings of the National Academy of Sciences* **110**, 7056–7061 (2013).
23. Mogilyansky, E. & Rigoutsos, I. The miR-17/92 cluster: a comprehensive update on its genomics, genetics, functions and increasingly important and numerous roles in health and disease. *Cell death and differentiation* **20**, 1603 (2013).
24. Hopp, K. *et al*. Functional polycystin-1 dosage governs autosomal dominant polycystic kidney disease severity. *The Journal of clinical investigation* **122**, 4257–4273 (2012).
25. Hajarnis, S., Lakhia, R., Patel, V.: MicroRNAs and polycystic kidney disease. (2015).
26. Lakhia, R *et al*. PPARA agonist fenofibrate enhances fatty acid β-oxidation and attenuates polycystic kidney and liver disease in mice. *American Journal of Physiology-Renal Physiology***:** ajprenal. 00352.02017, (2017).
27. Rakhshandehroo, M., Knoch, B., Müller, M. & Kersten, S.: Peroxisome proliferator-activated receptor alpha target genes. *PPAR research*, **2010** (2010).
28. Kersten, S., Desvergne, B. & Wahli, W. Roles of PPARs in health and disease. *Nature* **405**, 421 (2000).
29. Ling, C. *et al*. Epigenetic regulation of PPARGC1A in human type 2 diabetic islets and effect on insulin secretion. *Diabetologia* **51**, 615–622 (2008).
30. Bénit, P. *et al*. Large-scale deletion and point mutations of the nuclear NDUFV1 and NDUFS1 genes in mitochondrial complex I deficiency. *The American Journal of Human Genetics* **68**, 1344–1352 (2001).
31. Hoefs, S. J. *et al*. NDUFA2 complex I mutation leads to Leigh disease. *The American Journal of Human Genetics* **82**, 1306–1315 (2008).
32. Wakitani, S. *et al*. Multiple Acyl-CoA Dehydrogenation Deficiency (Glutaric Aciduria Type II) with a Novel Mutation of Electron Transfer Flavoprotein-Dehydrogenase in aCat. In: J*IMD Reports-Case and Research Reports, Volume 13*. Springer, pp 43–51 (2013).

33. Li, Y., Park, J.-S., Deng, J.-H. & Bai, Y. Cytochrome c oxidase subunit IV is essential for assembly and respiratory function of the enzyme complex. *Journal of bioenergetics and biomembranes* **38**, 283–291 (2006).
34. Mayr, J. A. *et al*. Mitochondrial ATP synthase deficiency due to a mutation in the ATP5E gene for the F1 ε subunit. *Human molecular genetics* **19**, 3430–3439 (2010).
35. Shimobayashi, M. & Hall, M. N. Making new contacts: the mTOR network in metabolism and signalling crosstalk. *Nature reviews Molecular cell biology* **15**, 155 (2014).
36. Ramanathan, A. & Schreiber, S. L. Direct control of mitochondrial function by mTOR. *Proceedings of the National Academy of Sciences* **106**, 22229–22232 (2009).
37. Zha, X., Sun, Q., Zhang, H.: mTOR upregulation of glycolytic enzymes promotes tumor development. Taylor & Francis (2011).
38. Zhu, P., Sieben, C. J., Xu, X., Harris, P. C. & Lin, X. Autophagy activators suppress cystogenesis in an autosomal dominant polycystic kidney disease model. *Human molecular genetics* **26**, 158–172 (2017).
39. Rowe, I. *et al*. Defective glucose metabolism in polycystic kidney disease identifies a new therapeutic strategy. *Nature medicine* **19**, 488 (2013).
40. Swenson-Fields, K. I. *et al*. Macrophages promote polycystic kidney disease progression. *Kidney international* **83**, 855–864 (2013).
41. Mun, H., Park, J. H.: Inflammation and Fibrosis in ADPKD. In: *Cystogenesis*. Springer, pp 35–44, (2016).
42. Chaulk, S. G. *et al*. Role of pri-miRNA tertiary structure in miR-17~92 miRNA biogenesis. *RNA biology* **8**, 1105–1114 (2011).
43. Chakraborty, S., Mehtab, S., Patwardhan, A. & Krishnan, Y. Pri-miR-17-92a transcript folds into a tertiary structure and autoregulates its processing. *Rna* **18**, 1014–1028 (2012).
44. de Pontual, L. *et al*. Germline deletion of the miR-17~92 cluster causes skeletal and growth defects in humans. *Nature genetics* **43**, 1026 (2011).
45. Han, Y.-C. *et al*. An allelic series of miR-17~92–mutant mice uncovers functional specialization and cooperation among members of a microRNA polycistron. *Nature genetics* **47**, 766 (2015).
46. Olive, V. *et al*. miR-19 is a key oncogenic component of mir-17-92. *Genes & development* **23**, 2839–2849 (2009).

Acknowledgements

We thank the UT Southwestern O'Brien Kidney Research Core Center (P30DK079328), the Mayo Translation PKD center (DK090728), UT Southwestern Bioinformatics core, Dr. Thomas Carroll (UT Southwestern), and Dr. Beth Levine (UT Southwestern) for providing critical reagents and services. We thank Dr. Silvia Ferrè (UT Southwestern) for helpful comments and discussion during the preparation of this manuscript. The work from the authors' laboratory is supported by National Institute of Health (R01DK102572) and the Department of Defense (D01 W81XWH1810673) to V.P. Vishal Patel have applied for a patent related to the treatment of polycystic kidney disease using miR-17 inhibitors. The Patel lab has a sponsored research agreement with Regulus Therapeutics. The remaining authors declare no conflict of interests.

Author Contributions

M.Y., R.L. and V.P. conceived the idea. M.Y., R.L., P.C.-S., and A.F. performed the experiments. M.Y. prepared the figures and wrote the manuscript with V.P.

Additional Information

Supplementary information accompanies this paper at https://doi.org/10.1038/s41598-019-38566-y.

Competing Interests: The authors declare no competing interests.

Publisher's note: Springer Nature remains neutral with regard to jurisdictional claims in published maps and institutional affiliations.